Asteroids, Comets, Meteors
Proceedings IAU Symposium No. 229, 2005
D. Lazzaro, S. Ferraz-Mello & J.A. Fernández, eds.

doi:10.1017/S1743921305006733

Trans–Neptunian objects' surface properties

M. A. Barucci[1] and N. Peixinho[1,2]

[1] LESIA-Observatoire de Paris, 92195 Meudon cedex, France
email: Antonella.Barucci@obspm.fr

[2] CAAUL, Observatório Astronómico de Lisboa, PT-1349-018 Lisboa, Portugal
email: peixinho@oal.ul.pt

Abstract. Recent observations in visible photometry have provided B, V, R and I high quality colors for more than 130 objects. Color diversity is now a reality in the TNOs population. Relevant statistical analyses have been performed and all possible correlations between optical colors and orbital parameters have been analyzed. A taxonomy scheme based on multivariate statistical analysis of a subsample of 51 objects described by the 4 color indices (B-V, V-R, V-I and V-J) has been obtained. A tentative interpretation of the obtained groups in terms of surface characteristics is given. Moreover, an extension of this taxonomy to the other 84 objects for which only three colors indices (B-V, V-R, and V-I) are available, is also presented.

The faintness of these objects limits the spectroscopic observations. Despite this, our group provided visible and infrared spectra for 18 objects using the Very Large Telescope (ESO, Paranal, Chile). The wavelength region ranging 0.4–2.3 microns encompasses diagnostic spectral features to investigate organic compounds, minerals and ices present on the surface of the TNOs. The investigation of the surface variation can be an identifier of possible composition diversity and/or different evolution with different physical processes affecting the surface.

The current knowledge of the surface properties and composition of the population will be presented, analyzed and interpreted.

Keywords. Trans-Neptunian Objects, Colors, Photometry, Spectroscopy, Surface composition

1. Introduction

Since the first discovery in 1992 (Jewitt & Luu 1993) the ice bodies located beyond the orbit of Neptune, are named Trans-Neptunian objects (TNOs) or Edgeworth Kuiper belt (EKB) objects. They are believed to represent the most pristine and thermally unprocessed objects of the Solar System that are accessible to ground based observations. They are presumed to be remnants of the external planetesimal swarms. More than 1000 objects have been detected to date and their number increases continuously. These objects can be divided dynamically in several classes: Classical, Resonants, Scattered and Extended scattering disk objects. Classical objects have orbits with low eccentricities and low inclinations and semi-major axes between about 42 and 48 AU; Resonants objects which are trapped in resonances with Neptune, the majority are located in or near the 3:2 mean motion resonance; Scattered objects have high-eccentricity, high-inclination orbits and a perihelion distance near q = 35 AU; while the Extended scattering disk objects are located out of interacting gravitational encounters with Neptune. Only two objects have been discovered up to date belonging this dynamical class: 2000 CR_{105} with semimajor axis at 224 AU, perihelion distance at 44 AU and aphelion at 401 AU; and 90377 Sedna with a semimajor axis at 501 AU and perihelion and aphelion distance at 76 and 927 AU, respectively. The Centaurs can also be associated with the TNO population. Centaurs seem to come from TNOs and are injected into their present orbit

by gravitational instabilities and collisions. With a less clear dynamical link, giant planets' irregular satellites may also originate from TNOs.

The study of physical and chemical properties of TNOs and Centaurs can provide essential information about the conditions present in the early Solar System environment. Studies of properties of these icy bodies are still limited by the faintness of these objects, even if observed with the world's largest telescopes. Knowledge about them is still very limited (see Barucci *et al.* 2004, for a review), particularly very few information is available on the compositional properties of their surfaces. Spectroscopy is the best method to investigate the surface composition of these remote objects however given their faintness, the visible and near-Infrared spectra are available only for few of them, and in general with very low S/N. Photometry is the only available technique which provides data for a large number of objects particularly in the visible region. Recent large programs have been carried out at Paranal (ESO, Chile) and at Mauna Kea (CFHT, Hawaii) by our group at the Paris Observatory and have provided excellent data on photometry and spectroscopy. Relevant statistical analyses have been performed and all possible correlations between optical colors and orbital parameters have been analyzed.

The analysis of color diversity is important for investigating surface composition diversity and for helping to understand the different evolution with different physical processes effecting the surface.

2. Photometry

Presently, given the faintness of TNOs, multicolor photometry is the most adequate observational technique to search for a statistically relevant characterization of these objects.

Several teams carried out statistical analysis of colors from their own observational surveys and/or compiled published data sets. Tegler & Romanishin (1998); Tegler & Romanishin (2000, 2003); Tegler *et al.* (2003), provided a BVR color data sample of 91 objects, representing one of the most relevant survey. Their works were at the origin of one the most intense debates in TNO surface properties. Another reference work was performed by Hainaut & Delsanti (2002). By compiling the available visible colors for 104 Minor Objects of the Outer Solar System (MBOSS), *i.e.* Centaurs, TNOs and comet nuclei, Hainaut & Delsanti (2002) published the first thorough statistical analysis in the field.

We will focus our discussion on the results and observational strategies from our team surveys, namely: a) The ESO Large Program (LP, PI = H. Boehnhardt): executed from April 2001 until March 2003, at VLT and NTT ESO telescopes, covering both visible/near–infrared photometry and spectroscopy. Visible BVRI colors for 71 objects and JHK colors for ∼20 objects were obtained under this program.

b) The Meudon Multicolor Survey (2MS, PI = A. Doressoundiram): started in 1997, using almost exclusively the CFHT telescope, with the aim of collecting an homogeneous set of color data, this program has obtained visible BVRI colors for another 71 objects.

2.1. *Specificities of TNO observations*

Typically, TNOs trail at a rate of $3''/hour$ (Centaurs trail typically at $6''/hour$). Therefore, exposure times have to be optimized to minimize trailing and maximize S/N ratio. Moreover, since TNOs rotate and may exhibit significant brightness variations in short time–scales (∼1 hour) colors should not be computed from exposures separated over too long of a time period. Since real simultaneous observations are generally impracticable,

https://doi.org/10.1017/S1743921305006733 Published online by Cambridge University Press

to derive quasi-simultaneous colors the filter photometric sequence $RVBIV$ is generally adopted. In some cases the same object is observed several times averaging their values.

Due to the faintness of TNOs, hence low S/N ratios, the use of classical photometry gives frequently large photometric errors and misestimated magnitudes. In order to maximize the S/N ratio the aperture correction (or growth-curve correction) technique is usually applied (Howell 1989; Stetson 1990). Additionally, since TNOs trail, the critical aperture radius below which the moving object aperture correction diverges from the untrailed stars by more than 1% are taken into account according to McBride *et al.* (1999).

2.2. *Absolute magnitude, phase effects and size estimation*

At any constant heliocentric and geocentric distance, an atmosphereless body presents a brightness increase with decreasing phase-angle (α). Phase effects vary smoothly and almost linearly for $10^\circ < \alpha < 90^\circ$. For lower α values an opposition effect occurs. For the case of TNOs phase angles are generally $\alpha < 2^\circ$ and the opposition effect plays a dominant role. Analysis of phase effects on TNOs (Sheppard & Jewitt 2002; Belskaya *et al.* 2003) have shown almost linear and fairly steep phase curves for the $0.2^\circ - 2^\circ$ phase angle range. With a phase curve slope ($\beta[mag/^\circ]$) modal value for TNOs of $\beta_{TNOs} = 0.14 \pm 0.03$ (Sheppard & Jewitt 2002) and a $\beta_{Centaurs} = 0.11 \pm 0.01$ for Centaurs, obtained from Bauer *et al.* (2002) data, the phase effect is to be regarded. We compute absolute magnitudes (H) from R–filter magnitudes using the linear approximation phase function $\phi(\alpha) = 10^{-0.4\beta\alpha}$, hence:

$$H_R = R - 5\,\log\,(r\Delta) - \beta\alpha \tag{2.1}$$

where R is the R–band calibrated magnitude, $r\,[AU]$ is the object's heliocentric distance, $\Delta[AU]$ is the object's geocentric distance, $\alpha[^\circ]$ is the phase angle during the observation and $\beta[mag/^\circ]$ is the phase curve slope. Diameters (D, in kilometers) are estimated using Russell (1916) equation:

$$D = 2\,\sqrt{\frac{2.24 \cdot 10^{16} \cdot 10^{0.4\,(R_\odot - H_R)}}{p_R}} \tag{2.2}$$

where $R_\odot = -27.1$ is the Sun's R–magnitude, H_R the object's absolute magnitude and p_R the geometric albedo in the R–band. Albedos for Centaurs and TNOs are still widely unknown. It has been standard procedure to use the average value for comet nuclei $p_R = 0.04$. However, after a few albedo measurements were available, Brown & Trujillo (2004) suggested $p_R = 0.09$ to be more adequate, so we opted this value in our most recent work. Recent analysis by Grundy *et al.* (2005) conclude a better median value of $p_R = 0.10$ or a mean value of $p_R = 0.14$. The uncertainties on size estimations are evidently high. Nevertheless, size has an albedo dependence of $D \propto 1/\sqrt{p_R}$, consequently if an albedo is underestimated by 50% sizes will be overestimated only by 25%.

3. Search for correlations

The minor bodies of the outer solar system are an immensely large population and can only be studied through samples. From the analysis of such data samples we attempt to infer general properties. One of the primary goals of the color survey was to search for any possible correlation between colors and orbital parameters. We used a statistical approach as the basic tool for our data analysis.

https://doi.org/10.1017/S1743921305006733 Published online by Cambridge University Press

3.1. *Hypothesis testing and its significance*

Statistical hypothesis testing is the well defined process of inferring from a sample whether or not a particular statement about the population appears to be true. Such statement is called *alternative hypothesis*, or H_1. The negation of this alternative hypothesis is called *null hypothesis*, or H_0. It is standard procedure to rate qualitatively the evidence against H_0 when discussing results, however not without controversy. Following the typical rough conventions in statistics, significance levels (SL) throughout this work may be read using the following rating:

$$\begin{cases} SL > 95\% & (\sim 2.0\sigma) & \text{— reasonably strong evidence against } H_0 \\ SL > 97.5\% & (\sim 2.2\sigma) & \text{— strong evidence against } H_0 \\ SL > 99\% & (\sim 2.5\sigma) & \text{— very strong evidence against } H_0 \end{cases}$$

3.2. *Trends and correlations*

Each objects is characterized by several surface colors and orbital parameters. The first and most basic statistical problem we are dealing with when confronted with two or more variables is to find if they are, or appear to be, in some way connected with each other. That is, if there is any trend between variables. The most common test for correlation is Pearson's correlation coefficient (r or r_p) and it has been used by Hainaut & Delsanti (2002). However, it has been common procedure to use its non-parametric equivalent Spearman ρ (or r_s), mainly because it it less sensitive to outliers and allows for very precise estimation of its significance level.

When a correlation value is significant it is often practical to discuss its intensity as ratings. Such is also a rough convention. The following ratings give a general idea of levels of intensity of possible Spearman ρ correlation values:

$$\begin{cases} 0.0 \leqslant \mid \rho \mid < 0.3 & \text{— absent/negligible correlation} \\ 0.3 \leqslant \mid \rho \mid < 0.6 & \text{— weak/moderate correlation} \\ 0.6 \leqslant \mid \rho \mid \leqslant 1.0 & \text{— strong correlation} \end{cases}$$

We have generated composite plots showing color, size, and orbital elements for the Centaurs and TNOs in our sample of 114 objects. Objects are plotted according to orbital eccentricity (e) *versus* semimajor–axis (a) and orbital inclination (i) *versus* semi–major axis (a) — Figs. 1 and 2, respectively. Surface colors are represented using the $B-R$ color index, which measures the ratio of the surface reflectance at B ($\sim 430\,nm$) and R ($\sim 660\,nm$) wavelengths. A color palette has been adopted to scale the color spread from neutral (solar like) colors $B-R=1.0$ (dark blue) to very red colors $B-R=2.0$ (red). To allow for a more clear color spreading, two objects possessing $B-R>2.0$ are indicated in black. The size of the symbols are proportional to the corresponding object's diameter (assuming a constant albedo of $p_R=0.09$) and a legend of size scales is also plotted. Orbital elements were obtained from *IAU Minor Planet Center*†. These two images condense all the trends under discussion here.

3.3. *Classical objects*

The first apparent trend in Fig. 1 is that Classical objects (semi–major axis between the 3:2 and 2:1 resonances) with perihelion distances beyond $40\,AU$ (*i.e.*, below the $q=40\,AU$ line) are mostly very red (Tegler & Romanishin 2000). Hainaut & Delsanti (2002) reported an explicit correlation between $B-R$ color and orbital eccentricity of $r_p=-0.57$ (Pearson's r). That is, with increasing eccentricity, hence diminishing of perihelion, Classical objects become bluer (Peixinho *et al.* 2004, hereafter PEI04) and

† `http://cfa-www.harvard.edu/iau/mpc.html`

https://doi.org/10.1017/S1743921305006733 Published online by Cambridge University Press

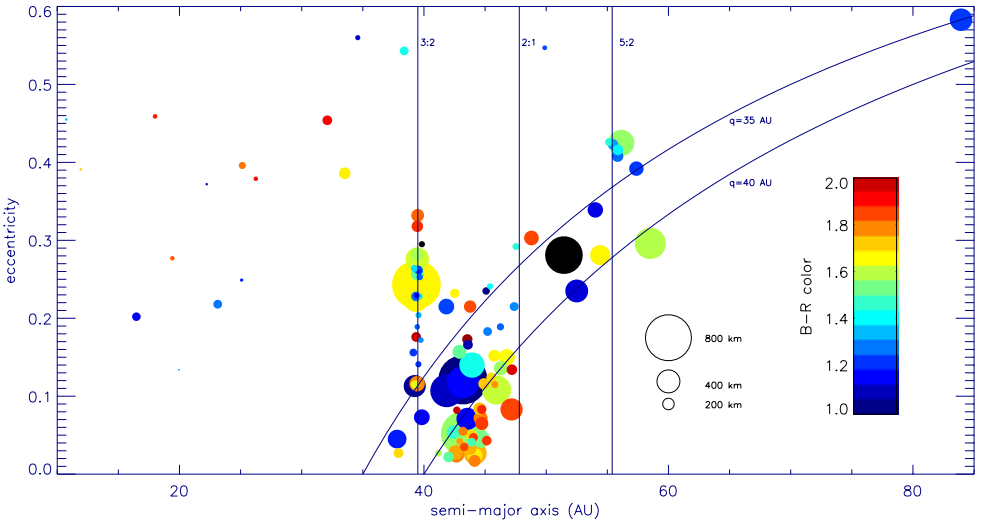

Figure 1. $B-R$ colors of Centaurs and TNOs from our survey for 114 objects in the orbital eccentricity *vs.* semi–major axis plane. Colors are scaled from blue (solar colors) to red (very red colors) indexed to the color palette on the right. Two very red objects are indicated in black. The sizes of the symbols are proportional to the corresponding object's diameter. The 3:2 ($a \sim 39.5\,AU$), 2:1 ($a \sim 48\,AU$) and 5:2 ($a \sim 55.4\,AU$) mean–motion resonances with Neptune are indicated. Perihelion curves for $35\,AU$ and $40\,AU$ are also marked. Figure adapted and updated from Doressoundiram *et al.* (2002).

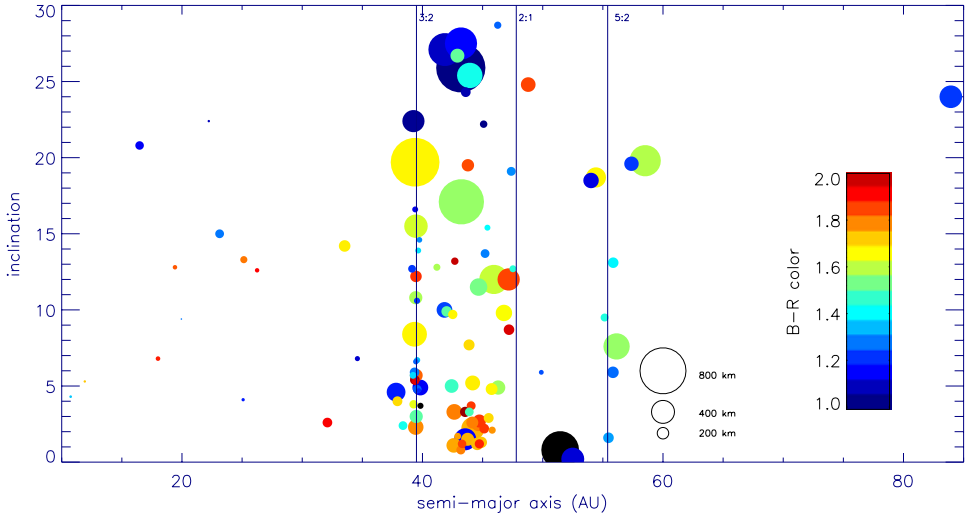

Figure 2. Same as Fig. 1 but for the orbital inclination *vs.* semi–major axis plane.

(Doressoundiram *et al.* 2005b, hereafter DOR05b) obtain $B-R$ color-perihelion correlations of $\rho = 0.52^{+0.05}_{-0.05}$ ($SL = 99.96\%$) and $\rho = 0.62$ ($SL = 99.98\%$) (Spearman's ρ), respectively. Such correlation is most probably connected with stronger solar surface processing (outgassing?) with shorter perihelia. Nevertheless, this color-q correlation is somewhat puzzling when confronted with Centaurs. No cometary activity has been detected

https://doi.org/10.1017/S1743921305006733 Published online by Cambridge University Press

among Classical objects, nonetheless they show a correlation between surface properties and perihelia. Centaurs, with much closer perihelia and detected cometary activity, do not. The answer may be in the collisional resurfacing model with triggered cometary activity proposed by (Delsanti *et al.* 2004, hereafter DEL04) . Object resurfacing is not only caused by collisional resurfacing but also by the subsequent sublimation of freshly exposed volatiles, which strongly depends on perihelion. Additionally, PEI04 report a H_R dependence (or size if we assume an homogeneous or quasi–homogeneous albedo) of the color-q correlation. Intrinsically brighter (larger) Classical objects exhibit a much stronger color-q correlation. DEL04 model predicts that objects large enough to retain a bound coma (*i.e.*, $D > 100\ km$ assuming $p_R = 0.09$) should be more efficient in rejuvenating their surfaces. Moreover, Lacerda & Luu (2005), based on an analysis of rotational properties of TNOs conclude that objects with

$D < 270\ km$ (assuming $p_R = 0.09$) are better explained as by-products of the collisional evolution. Those with $D > 270\ km$ can be "rubble-piles" which have survived to collisional evolution. Given the correlation results it would be interesting to study if the by-products of the collisional evolution are also less rich in volatiles, hence less efficient in resurfacing.

From the representation with orbital inclination (Fig. 2) we may observe the tendency for Classical objects to be bluer and larger with inclination. The color-inclination trend was first reported by Tegler & Romanishin (2000) and the first explicit correlation values were obtained by Trujillo & Brown (2002); Hainaut & Delsanti (2002); Doressoundiram *et al.* (2002). Levison & Stern (2001) reported a possible size–inclination trend, recently confirmed by Trujillo & Brown (2003); Bernstein *et al.* (2004). Moreover, Levison & Stern (2001); Brown (2001) claimed the existence of two inclination populations among the TNOs: one primordial and dynamically "cold" and another dynamically "hot" probably superimposed.

Based on an analysis of color variance in function of inclination, PEI04 shows that the dynamically "cold" population defines a red cluster of objects for $i < 4.5°$. However, it could extend until $i < 12.0°$. Gomes (2003) proposed a migration model under which the two populations have different origins. Gomes' work distinguishes the disk of primordial objects being scattered by Neptune during its outwards migration in inner disk and outer disk. At the end of the migration phase the inclination distribution of TNOs will result from the superposition of the inner disk objects with highly inclined orbits ("hot" population) into the outer disk objects. The latter maintain their low inclined orbits ("cold" population).

In a nebula whose surface density decreases with heliocentric distance, the size of the largest objects also decrease. Objects formed in the inner disk should be larger than those formed in the outer disk — nevertheless, a population of smaller objects as a result of disruptive collisions should coexist. In the less denser outer regions, collisional evolution should be less significant. Hence, outer disk objects should be more affected by space weathering, exhibiting redder surfaces, while inner disk objects should be more affected by collisional resurfacing, exhibiting bluer surfaces. Inner disk objects may have different compositions, hence different colors. Such reasonings could explain both color–inclination and H_R–inclination trends found for Classical objects (Tegler *et al.* 2003; Morbidelli *et al.* 2003).

Nevertheless, Gomes' model predicts an inclination-eccentricity distribution for Plutinos, in function of their inner or outer disk origin, that when confronted with their color distribution does not seem compatible with the previous reasoning (PEI04). The color-q correlation is still present in the "hot" Classical objects, whereas the color-inclination correlation seems to be a masking effect of the previous one (PEI04). These results,

https://doi.org/10.1017/S1743921305006733 Published online by Cambridge University Press

although obtained with small sub-sampling, suggest that the color distribution of Classical objects cannot be exclusively due to eventual intrinsic differences.

3.4. *Plutinos*

Plutinos (objects in the 3:2 resonance) appear to lack any trends between surface colors and orbital parameters. Consequently, processes connected with the color-eccentricity/perihelion and color-inclination trends found for Classical objects seem absent among Plutinos. There is an apparent excess of intrinsically faint (small) blue Plutinos. However, such excess does not result in a significant color-size correlation (Hainaut & Delsanti 2002, PEI04). From the works by Thébault & Doressoundiram (2003) on the collisional resurfacing scenario (Luu & Jewitt 1996a), one of the major drawbacks of such a model was a prediction for a lack of red Plutinos. However, the collisional resurfacing scenario with triggered cometary activity (DEL04) predicts a more efficient surface rejuvenation for larger objects, contrary to what is observed among Plutinos. This subject needs further investigation.

3.5. *Scattered disk objects*

SDOs (eccentric orbits beyond the 2:1 resonance and also those above the $q = 35\,AU$ line) are one of the most undersampled families. Up to date no significant color-orbital correlations have been found for this class. However, Tegler *et al.* (2003) and PEI04 report that SDOs display a lack of very red surfaces. Moroz *et al.* (2003) demonstrate that different components transform neutral (blue) surface colors into red and further to neutral. Given the typically high aphelion values for SDOs, they are exposed to more intense irradiation dosages (Cooper *et al.* 2003) and their bluer colors may be due to ion irradiation saturation. Such results suggest that the present collisional resurfacing models are too simplified

(Strazzula *et al.* 2003).

3.6. *Centaurs*

Centaurs show evidence for a color-eccentricity correlation that does not translate into a color-perihelia correlation (PEI04). There is no obvious interpretation for such trend. However, they subdivide in two color groups. Such puzzling result is discussed in the next section.

3.7. *Bimodality versus Unimodality*

The Centaurs' and TNOs' color distribution has always been very controversial. Tegler & Romanishin (1998); Tegler & Romanishin (2000) reported the identification of two separated color groups for Centaurs and TNOs (mixed together). Other works claimed a continuous color spreading (e.g. Barucci *et al.* 2000, 2001; Jewitt & Luu 2001; Doressoundiram *et al.* 2001; Hainaut & Delsanti 2002). With a new and exhaustive statistical analysis Tegler & Romanishin (2003) — hereafter TR03 — apparently solved the two color controversy.

Peixinho *et al.* (2003), hereafter PEI03, reanalyzing TR03's data sample conclude that mixing both Centaurs and TNOs lead to the erroneous conclusion of a global bimodality, while there is no evidence for two visible color groups in the TNOs population alone. Using Dip Test (Hartigan & Hartigan 1985), from a compiled sample of 20 quasi–simultaneous $B - R$ colors, PEI03 shows that Centaurs divide in two groups with a significance of 99.5%. Such a possibility had already been highlighted by Boehnhardt *et al.* (2001). When removing Centaurs from TR03 sample, significance level for bimodality is on the order $\sim$55% much below the minimum 95%.

https://doi.org/10.1017/S1743921305006733 Published online by Cambridge University Press

In a latter work Tegler *et al.* (2003) confirm these findings, whereas Mueller *et al.* (2004) — discussing Bauer *et al.* (2003) VRI data for 24 Centaurs — states that this bimodality is not apparent in the VRI color range. Hence, it appears that without the $B-V$ color information the two groups cannot be (easily) distinguished.

Centaurs are presumed to originate among TNOs, although its specific origin is still in debate (Levison & Duncan 1997; Yu & Tremaine 1999). Hence it is physically difficult to understand the existence of these two color groups. It is possible that TNOs possess real intrinsic differences, even if there is no evidence against a continuous spread of visible colors — we will return to this subject in Section 5. Since Centaurs occupy less denser regions and experience fewer collisions, DEL04's model actually produces two color groups among Centaurs, even with a continuos color spreading of TNOs. The model predicts much more red Centaurs than blue ones and considered Centaurs as "native" residents with stable orbits, which is not the case. The mean Centaur's half-live is $\sim$2.76 Myr and one TNO is expected to enter the Centaur region every $\sim$125 yr (Horner *et al.* 2004). More detailed simulation should be carried out in order to understand this behavior.

4. Comparing color distributions

The question of the origins of the several dynamical groups of TNOs and their presumably related populations is still an open debate. Identifying the color distribution compatibilities/incompatibilities, *i.e.* color distribution differences, between each population is a first step to establish their "genetic" links.

Hainaut & Delsanti (2002), from their compiled MBOSS data-sample, had found that: (a) short period comets' (SPCs) colors are incompatible with those of Classical objects, Plutinos and Centaurs, but only marginally incompatible with SDOs; and (b) Plutinos, Classical objects and SDOs do not evidence color incompatibility between them. Jewitt (2002) also reported that the cometary nuclei were bluer than TNOs.

DOR05b, with a different statistical approach analyses the $V-R$ color (in)compatibilities using: (a) LP+2MS data samples for Centaurs and TNOs; (b) Lamy *et al.* (2005) compiled colors of SPC; and (c) colors compiled from the literature of giant planets' irregular satellites. Furthermore, given the lack of strict dynamical definitions for most families of TNOs, two different classifications schemes of Classical objects and SDOs were considered. Peixinho (2005) extends this work including also LP data leading, basically, to coincident conclusions. Apart some subtleties from the two classification schemes (see DOR05b), results may be simplified as:

(a) SPCs: compatible with irregular satellites and marginally incompatible with SDOs.
(b) Irregular satellites: compatible with SDOs and SPCs.
(c) Centaurs: compatible with all families of TNOs, in spite of their bimodal colors.
(d) Plutinos: compatible with SDOs, Centaurs and Classical objects
(e) Classical objects: only compatible with Centaurs and Plutinos.
(f) SDOs: compatible with all classes except with Classical objects and possibly with SPCs.

The differences of trends among each dynamical class of TNOs (SDOs, Plutinos and Classical objects) and Centaurs may be caused by different surface processing. Such eventual processing does not appear to be sufficiently strong to induce color incompatibility between Plutinos and Centaurs with SDOs or with Classical objects. Nevertheless, the incompatibility between SDOs and Classical objects indicates that the red cluster of

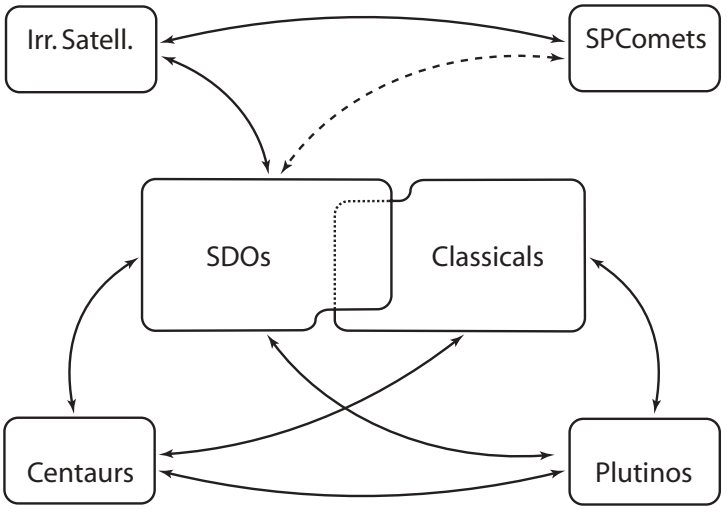

Figure 3. Diagram for Peixinho (2005) and DOR05b's colors compatibility between families. Solid arrows indicate relations between those populations with no evidence for incompatibility, *i.e.*, color compatible populations. Dashed arrows indicate relations with borderline evidence for incompatibility, *i.e.*, possible color (in)compatible families. At the center of the image SDOs and Classicals, which are not compatible, are represented with an overlap to evidence the classification uncertainty of some objects.

"cold" Classical objects may have a different origin. Note, however, that such study was performed only with one color index.

It comes as a surprise that SPCs are not clearly compatible with SDOs and are incompatible with Centaurs, their presumed precursors. Some process modifies SPCs' surfaces when entering into the inner solar system. Jewitt (2002), who had noticed a lack of very red surfaces among SPCs, proposed a surface alteration process in which the formation of a rubble mantle of debris (non-ejected by sublimating stages) or a ballistic mantle (ballistic redeposition of ejected debris) may resurface the object. Considering the irradiation mantles of TNOs as sublimation inhibitors that can be blown off when reaching short perihelion distances, TNOs, with any surface colors, may become Centaurs that will become blue or red, according to the DEL04's model and while migrating to become SPCs loose their irradiation mantles and suffer a complete resurfacing. Under this scenario the color compatibilities of irregular satellites would be the expected ones.

Tegler *et al.* (2003), on the other hand, from a dichotomized $B - R$ color pattern analysis of Centaurs and TNOs conclude a consistency with a primordial origin of their surface colors. Simple dynamical evolution, without post-formation surface evolution of colors, appear also to be a viable approach. The lack of multicolor observations for some parts of the EKB, the low significancy of several color correlations and the incapability of the current dynamical and surface evolution models to reproduce some of the observed trends make this subject an open question.

5. Taxonomy

Dealing with a large number of objects it is important to distinguish groups of objects with similar surface properties. Such approach to study physical properties of asteroids was resulted in taxonomy scheme based mostly on surface colors and albedos which became an efficient tool in asteroid investigations. (Barucci *et al.* 2005a, hereafter BA05)

https://doi.org/10.1017/S1743921305006733 Published online by Cambridge University Press

Table 1. The average colors (B-V, V-R, V-I, V-J) and the relative standard deviation for the four taxonomic groups obtained by the G-mode on the sample of 51 objects. The V-H has been computed analyzing the subset of 37 objects.

Class	B-V	V-R	V-I	V-J	V-H
BB	0.70±0.04	0.39±0.03	0.77±0.05	1.16±1.17	1.21±0.52
BR	0.76±0.06	0.49±0.03	0.9±0.07	1.67±0.19	2.04±0.24
IR	0.92±0.03	0.61±0.03	1.20±0.04	1.88±0.09	2.21±0.06
RR	1.08±0.08	0.71±0.04	1.37±0.09	2.27±0.20	2.70±0.24

applied to the 51 TNOs and Centaurs described by the 4 color indices B-V, V-R, V-I and V-J the same statistical analysis used in the '80s to classify the asteroid population: the multivariate statistic analysis (G-Mode) from Barucci *et al.* (1987) and the Principal Component Analysis (Tholen 1984; Tholen & Barucci 1989). BA05 considered all the high quality available colors on TNOs and Centaurs published. They analyzed: i) a set of data for 135 objects observed in B, V, R and I band, ii) a set of 51 objects observed in B, V, R, I, J bands with high quality homogeneous data and iii) a sub-sample of 37 objects also including H band. They selected as a primary sample for the analysis a complete and homogeneous set of 51 objects observed in five filters (B, V, R, I, J), adopting the mean values weighted with the inverse of the error of individual measurement when multiple observations of an object were available. The results of this analysis show that the first principal component (PC1) accounts for most of the variance of the sample (94%) with high weight of V-J (46%). PC2 adds less than 5% to the total variance. Most of the information is concentrated on PC1 which shows four peaks at high density with objects having a neutral color with respect to the Sun (lower PC1 scores) toward the reddest objects of the solar system (higher PC1 scores). As the relationship between the variables is probably not linear, BA05 used a powerful multivariate statistical grouping method (G-mode) to recognize the structure of the found distribution. The G-mode method allows the user to obtain an automatic classification of a statistical sample containing N objects described by M variables (for a total of $M \times N$ degrees of freedom, the d.o.f. number must be >100) in terms of homogeneous taxonomic groups. The method has no a priori grouping criteria, takes into account the instrumental errors in measuring each variable, and also gives indications on the relative importance of the variables in separating the groups. Using the G-mode, a sample of 51 objects and B-V, V- R, V-I and V-J colors were taken as variables ($51 \times 4 = 204$ d.o.f.) and used for the analysis. Using a high confidence level Q (corresponding to 3σ), four homogeneous groups have been obtained. The weight of each variable in separating these groups is 32% for the V-I color, 26% for the V-R, 22% for V-J and 20% for B-V implying that all variables contribute to define the obtained four groups. In Table 1, the color average value and the relative standard deviation for each group are given. The obtained groups are represented in two complementary three dimensional plots (Fig. 4) for the B-V, V-R, V-I and (Fig. 5) for the B-V, V-R, V-J color spaces. The different behavior of the four classes is clearly shown, as well as the role of each color (and particularly V-I and V-J) in assigning the samples to each group. One object, 2000 OK67, does not belong to any group. Moreover, BA05 analyzed a subset of 37 objects for which the V-H color is also available. G-mode analysis applied to this sub-sample described by 5 colors (for a total of $37 \times 5 = 185$ degrees of freedom) provides practically the same well determined four groups. The same objects fall in the same group obtained with 4 variables.

https://doi.org/10.1017/S1743921305006733 Published online by Cambridge University Press

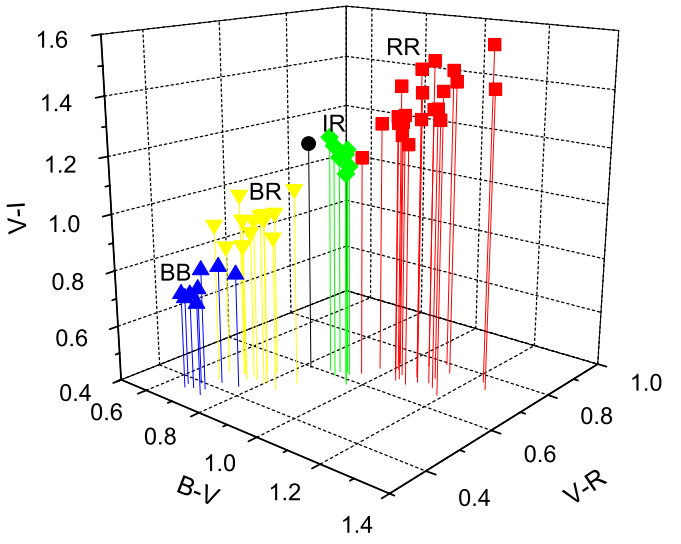

Figure 4. The plot shows the groups in the three dimensional space: B-V, V-R, V-I. Different symbols-colors represent different classes. The black dot represents the objects 2000 OK_{67} which is not belonging to any group.

5.1. *The four obtained classes*

On the basis of this analysis, a taxonomy of TNOs and Centaurs based on their surface broadband colors has been proposed. A two-letter designation of the found groups is introduced to distinguish TNO taxonomy from the asteroid taxonomy. Objects having a neutral colors with respect to the Sun are classified as BB ("blue") group, those having a very high red color are classified as RR ("red"). The BR group consists of objects with an intermediate blue-red color while IR group includes moderately red objects. 2000 OK67, which the G-mode lefts out of this scheme, might be considered as a "single object group". The assignment of each object to one of these groups is reported in the last column of Table 2.

5.2. *Extended taxonomy*

The G-mode has been extended (Fulchignoni *et al.* 2000) to assign to one of the already defined taxonomic groups any object for which the same set of variables become available. Moreover, even if a subset of the variables used in the initial development of the taxonomy is known for an object, the algorithm allows us to give at least a preliminary indication of its appurtenance to a given group. The lack of information on a variable is reflected by the fact that an object could be assigned to two different classes when the lacking variable is the one which operates the discrimination between these classes. The algorithm has been adopted to each of the 84 other TNOs for which the B-V, V-R and V-I colors are available. The obtained preliminary classification for these objects is also reported on the bottom half of Table 2. The appurtenance to a given group has to be considered always with some caution because it is only an indication obtained with an incomplete data set. A double assignment has been obtained for 13 objects, and 15 objects are not classified at all.

https://doi.org/10.1017/S1743921305006733 Published online by Cambridge University Press

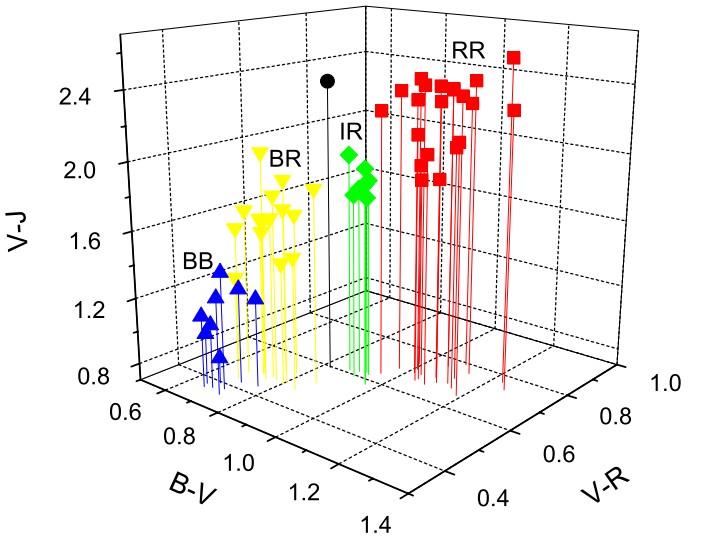

Figure 5. The plot shows the groups in the three dimensional space: B-V, V-R, V-J. Different symbols-colors represent different classes. The black dot represents the objects 2000 OK_{67} which is not belonging to any group.

5.3. *Groups interpretation*

The four groups found by G-mode analysis seem well defined and homogeneous in color properties. The RR group contains the reddest objects of the Solar System. Some well observed objects are members of this group like, 5145 Pholus, 47171 (1999 TC_{36}), 55576 (2002 GB_{10}), 83982 (2002 GO_9) and 90377 Sedna. All these objects seem to contain a few percent of H_2O ice on the surface. The reddeness of the group could imply a large amount on the surface composition of Titan tholin and/or ice tholin. Tholins are complex organic solids produced by the irradiation. The BB group contains objects having a neutral reflectance spectra. Typical objects of the group are 2060 Chiron, 90482 Orcus, 19308 (1996 TO_{66}) and 15874 (1996 TL_{66}). The typical spectra is flat, somewhat bluish in the NIR. The H_2O absorption bands seems generally stronger than in the other groups, although the H_2O ice presence in the Chiron spectrum seems connected to temporal/orbital variations, and the spectrum of 1996 TL_{66} is completely flat. The presence of large amount of amorphous carbon seems common to the members of this group. The IR group is less red than RR group. Typical members of this class are 20000 Varuna, 38628 Huya, 47932 (2000 GN_{171}), 26375 (1999 DE_9) and 55565 (2002 AW_{197}). Three of these objects seem to contain hydrous silicates on the surface. The BR group is an intermediate group between BB and IR even if its color is closer to the behavior of IR group. The typical members of this class are 8405 Asbolus, 10199 Chariklo, 54598 Bienor and 32532 Thereus. A few percent of H_2O is present on the surface of these objects but for Asbolus, Romon-Martin *et al.* (2002) did not find any ice absorption features during its complete rotational period. Passing from neutral (BB group) to very red (RR group) spectra, a higher content of organic material is required to fit appropriately the characteristic spectrum of the single object. Groups BB and BR in general do not require the presence of organic materials or only few percent is needed to achieve their color. H_2O ice may be present in all spectra of the groups. The groups BB and BR have color spectra

https://doi.org/10.1017/S1743921305006733 Published online by Cambridge University Press

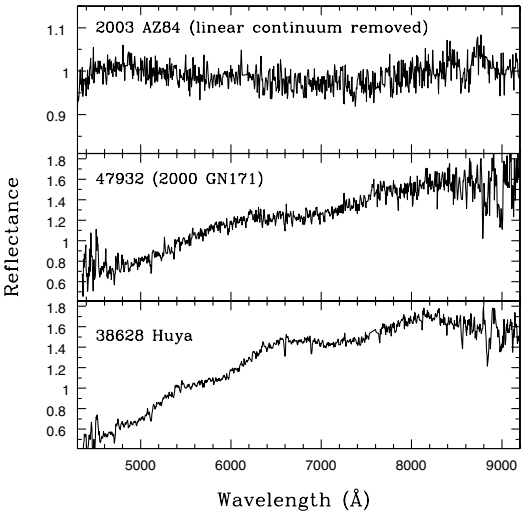

Figure 6. Visible spectra of three TNOs showing aqueous alteration absorption bands. The top spectrum of 2003 AZ84 has been obtained removing the continuum computed with a linear least squares fit to the smoothed spectral data (Fornasier *et al.* 2004). The other two have been obtained by (Lazzarin *et al.* 2003).

very similar to those of C-type and D-type asteroids. Unfortunately we can not associate an albedo range to each taxonomic group because of the lack of albedo data. The few available determinations based from ground observations are very uncertain and do not show any trend with the different classes.

6. Spectroscopy data

Broadband color photometric can provide rough information on the surface of the atmosphereless objects, but the most detailed information on their compositions can be acquired only from spectroscopic observations, especially in the near-infrared spectral region. Most of the known TNOs and Centaurs are too faint for spectroscopic observations, even with the world's largest telescopes, and so far only the brightest bodies have been observed by spectroscopy. The limiting magnitude at the present time, even if observing with 8-10 m telescopes, is about $V = 23$ mag. The exposure time required is generally long and as the objects rotate around their principal axis the resulting spectra probably arise from signals from both sides of the object. Reflectance spectroscopy (covering the wavelength range between 0.4 and 2.4 μm) provides the most sensitive technique to characterize the major mineral phases and ices present on TNOs. Visible and near-infrared spectroscopy allow us to investigate the presence of the silicate minerals like pyroxene, olivine, and sometimes feldspar, as well as primitive carbonaceous assemblages, and organic tholins. The near infrared region is very important to diagnose the presence of ices and/or hydrocarbons. Weakly active Centaurs or TNOs could show fluorescent gaseous emission bands.

https://doi.org/10.1017/S1743921305006733 Published online by Cambridge University Press

Table 2. On the top, the selected sample of 51 objects and the proposed taxonomical classification based on four color indices (B-V, V-R, V-I, and V-J) are listed. Preliminary classification for the other 84 objects based only on three color indices (B-V, V-R, and V-I) are reported after the separation line.

Object	G-mode class	Object	G-mode class
2060 Chiron	BB	38628 Huya	IR
5145 Pholus	RR	40314 1999 KR_{16}	RR
7066 Nessus	RR	44594 1999 OX_3	RR
8405 Asbolus	BR	47171 1999 TC_{36}	RR
10199 Chariklo	BR	47932 2000 GN_{171}	IR
10370 Hylonome	BR	48639 1995 TL_8	RR
15788 1993 SB	BR	52975 Cyllarus	RR
15789 1993 SC	RR	54598 Bienor	BR
15820 1994 TB	RR	55565 2002 AW_{197}	IR
15874 1996 TL_{66}	BB	55576 2002 GB_{10}	RR
15875 1996 TP_{66}	RR	58534 1997 CQ_{29}	RR
19299 1996 SZ_4	BR	60558 2000 EC_{98}	BR
19308 1996 TO_{66}	BB	63252 2001 BL_{41}	BR
19521 Chaos	IR	79360 1997 CS_{29}	RR
20000 Varuna	IR	83982 2002 GO_9	RR
24835 1995 SM_{55}	BB	90377 Sedna	RR
24952 1997 QJ_4	BB	90482 Orcus	BB
26181 1996 GQ_{21}	RR	91133 1998 HK_{151}	BR
26308 1998 SM_{165}	RR	1996 TQ_{66}	RR
26375 1999 DE_9	IR	1996 TS_{66}	RR
29981 1999 TD_{10}	BR	1998 WU_{24}	BR
32532 Thereus	BR	1999 CD_{158}	BR
32929 1995 QY_9	BR	2000 OJ_{67}	RR
33128 1998 BU_{48}	RR	2000 OK_{67}	—
33340 1998 VG_{44}	IR	2000 PE_{30}	BB
35671 1998 SN_{165}	BB		
15760 1992 QB_1	RR	1996 RR_{20}	RR
15810 1994 JR_1	—	1996 TK_{66}	RR
15836 1995 DA_2	—	1997 QH_4	RR
15883 1997 CR_{29}	BR	1997 RT_5	—
16684 1994 JQ_1	RR	1998 KG_{62}	IR-RR
19255 1994 VK_8	RR	1998 UR_{43}	BR
28978 Ixion	IR-RR	1998 WS_{31}	BR
31824 Elatus	RR-IR	1998 WT_{31}	BB
33001 1997 CU_{29}	RR	1998 WV_{31}	BR
38083 Rhadamanthus	BR	1998 WZ_{31}	BB-BR
38084 1999 HB_{12}	BR	1998 XY_{95}	RR
42301 2001 UR_{163}	—	1999 CB_{119}	RR
49036 Pelion	BR	1999 CF_{119}	BR
52872 Okyrnoe	BR	1999 CX_{131}	RR
55636 2002 TX_{300}	BB	1999 HC_{12}	BR
59358 1999 CL_{158}	BB-BR	1999 HR_{11}	—
60454 2000 CH_{105}	RR	1999 HS_{11}	RR
60608 2000 EE_{173}	IR	1999 OE_4	RR
60620 2000 FD_8	RR	1999 OJ_4	RR
60621 2000 FE_8	BR	1999 OM_4	RR
66452 1999 OF_4	RR	1999 RB_{216}	BR
69986 1998 WW_{24}	BR	1999 RE_{215}	RR
69988 1998 WA_{31}	BR	1999 RX_{214}	RR-IR
69990 1998 WU_{31}	—	1999 RY_{214}	BR
79978 1999 CC_{158}	IR-RR	1999 XX_{143}	RR
79983 1999 DF_9	RR	2000 CL_{104}	RR
82075 2000 YW_{134}	BR	2000 FZ_{53}	—
82158 2001 FP_{185}	—	2000 GP_{183}	BB-BR
85633 1998 KR_{65}	RR	2001 CZ_{31}	BR
86047 1999 OY_3	BB	2001 KA_{77}	RR
86177 1999 RY_{215}	BR	2001 KD_{77}	RR
91205 1998 US_{43}	BR	2001 KP_{77}	—
91554 1999 RZ_{215}	—	2001 KY_{76}	—
95626 2002 GZ_{32}	BR	2001 QF_{298}	BB
1993 RO	IR-RR	2001 QY_{297}	BR
1993 FW	RR-IR	2001 UQ_{18}	RR
1994 ES_2	—	2002 DH_5	BR-BB
1994 EV_3	RR	2002 GF_{32}	RR
1994 TA	RR	2002 GH_{32}	—
1995 HM_5	BR	2002 GJ_{32}	—
1995 WY_2	RR-IR	2002 GP_{32}	—
1996 RQ_{20}	IR-RR	2002 GV_{32}	RR

https://doi.org/10.1017/S1743921305006733 Published online by Cambridge University Press

6.1. *Visible spectra*

The visible spectra are generally featureless with a difference in the spectral gradient, ranging from neutral to very red. Pholus and Nessus are the reddest objects known up to now in the Solar System.

The visible wavelength is also an important region and can be used to infer information on the composition, particularly for the especially "red" objects, whose reflectance increases rapidly with wavelength and can be associated to the presence of organic material on their surface. The visible range is also important to detect aqueous altered minerals like for example phyllosilicates.

Few objects (see Fig. 6) have broad absorptions present in their spectra. In the spectrum of 47932 (2000 GN_{171}), an absorption centered at around 0.7μm has been detected with a depth of ∼8%, while in the spectrum of 38628 (2000 EB_{173}) two weak features centered at 0.6μm and at 0.745μm have been detected with depths of ∼7% and 8.6%, respectively (Lazzarin *et al.* 2003; de Bergh *et al.* 2004). The spectrum of 2003 AZ_{84} also seems to show a weak absorption centered around 0.7μm and extending from 0.5 to 0.85μm with a depth of about 3% as respect to the continuum (Fornasier *et al.* 2004). These features are very similar to those due to aqueously altered minerals, found in some main belt asteroids (Vilas & Gaffey 1989, and subsequent papers) and are attributed to an $Fe^{2+} \rightarrow Fe^{3+}$ charge transfer in iron oxides in phillosilicates. How this aqueous alteration process might have effects so far from the Sun is not well understood, but it cannot be excluded that hydrated minerals could have been formed directly in the early solar nebula. Finding aqueous altered materials in TNOs is not too surprising (de Bergh *et al.* 2004) since hydrous materials seem to be present in comets, and hydrous silicates are detected in interplanetary dust particles (IDPs) and in micrometeorites.

6.2. *Near-infrared spectra*

The near-infrared wavelength region carries signatures from water ice (1.5, 1.65, 2.0 μm), other ices (CH_4 around 1.7 and 2.3 μm, CH_3OH at 2.27 μm, and NH_3 at 2 and 2.25 μm), and solid C-N bearing material at 2.2 μm.

The first observed Centaurs were 2060 Chiron and 5145 Pholus (see Barucci *et al.* 2002b, for a reviw on Centaurs) while the first spectrum of a TNO 15789 (1993 SC) was observed by Luu & Jewitt (1996b) in the visible and by Brown *et al.* (1997) in the NIR showing a very noisy reddish spectrum with some features which may be due to hydrocarbon ice (see Barucci *et al.* 2004, for TNO general review).

In the infrared region some spectra are featureless, while others show signatures of water ice, and methanol or other light hydrocarbon ices. Very few of these objects have been well studied in both visible and near infrared and rigorously modeled. In fact these objects are faint and even observations with the largest telescopes (Keck and VLT) do not generally yield good quality spectra. The TNOs are even fainter than Centaurs, and in both cases only few spectra are available, generally with very low S/N. The spectra of TNOs and Centaurs have common behaviour and their surface characteristics seem to show wide diversity. Interpretation is also very difficult because the behavior of models of the spectra depends on the choice of many parameters. In Fig. 7 and 8 we report the visible and NIR spectra for all the objects (9 Centaurs and 9 TNOs) observed at VLT (ESO, Chile) with the best model computed fitting of the data.

6.3. *Surface composition*

Radiative transfer models have been used to interpret the V+NIR spectra of TNOs and Centaurs and several attempts have been performed by modelling the surface composition of these objects with intimate or geographical mixtures of organics, ices and minerals.

https://doi.org/10.1017/S1743921305006733 Published online by Cambridge University Press

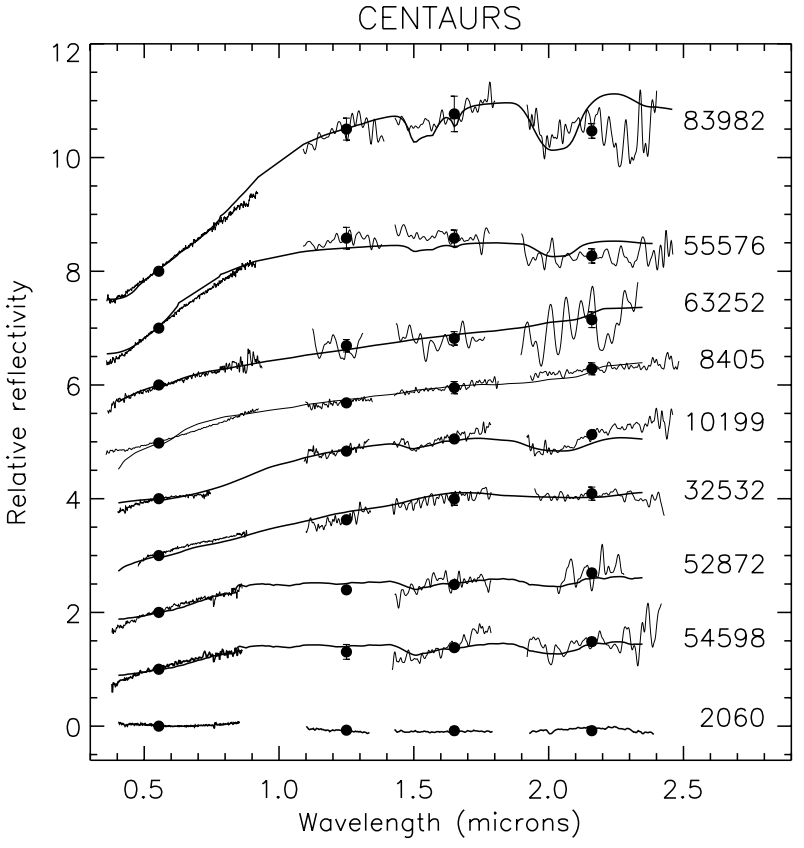

Figure 7. Visible and near-infrared spectra of Centaurs observed at VLT (ESO). The dots represent the B, V, R, I, J, H and K colors, used to adjust the spectral range. The continuous lines superimposed to the spectra are the best-fit models suggested for the surface composition of each objects. All the spectra are normalize at 0.55μm and are shifted by one unit for clarity. The spectra and models are 83982 & 55576 (Doressoundiram *et al.* 2005a); 63252 (Doressoundiram *et al.* 2003); 52872 & 54598 (Dotto *et al.* 2003c); 8405 Romon-Martin *et al.* (2002); 10199 (Dotto *et al.* 2003a); 32532 (Barucci *et al.* 2002a); 2060 (Romon-Martin *et al.* 2003).

The red spectral slopes are in general well reproduced supposing the presence on the surface of organic compounds like tholins or kerogens. Low albedo objects can be well modelled with a high percentage of amorphous carbon. Silicates seem also to be present like the olivine for example on the surface of 5145 Pholus (Cruikshank *et al.* 1998). Water ice is not present in all objects even if ices are the predominant constituent of these distant objects. In Fig. 7 and 8 the computed model is overlapped on the observed spectra. The models present the best current fit to the data, even if they are not unique and depend on many parameters like albedos, different percentages of mixtures and grain size composants. The spectrum of (63252) 2001 BL_{41}, (26181) 1996 GQ_{21} (Doressoundiram *et al.* 2003) and (8405) Asbolus (Romon-Martin *et al.* 2002) are modeled with geographical mixtures of tholins, ice tholin, amorphous carbon. The spectrum of (10199) Chariklo (Dotto *et al.* 2003c) is modeled with a geographical mixture of tholins, amorphous carbon and water ice. Those of (52872) Okyrhoe (1998 SG_{35}) and (54598) 2000 QC_{243} are modeled with geographical mixtures of kerogen, olivine and water ice (Dotto *et al.* 2003b). The spectra of (47171) 1999 TC_{36} (Dotto *et al.* 2003b), (28978) Ixion (Boehnhardt *et al.*

https://doi.org/10.1017/S1743921305006733 Published online by Cambridge University Press

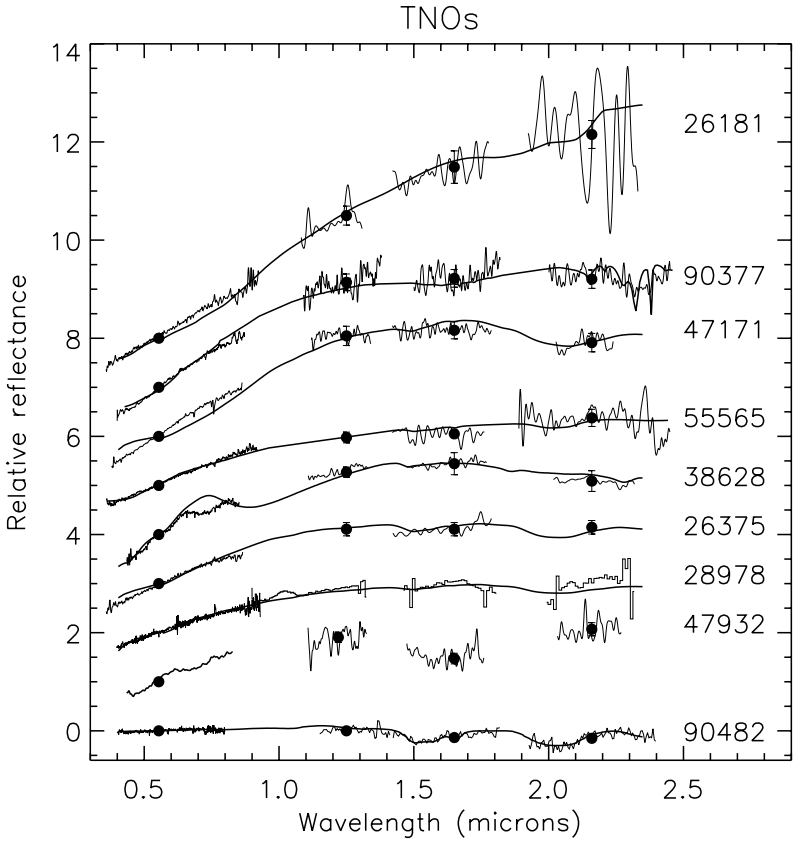

Figure 8. Visible and near-infrared spectra of TNOs observed at VLT (ESO, except the NIR of 28978 that has been observed at TNG (La Palma). The dots represent the B, V, R, I, J, H and K colors, used to adjust the spectral range. The continuous lines superimposed to the spectra are the best-fit models suggested for the surface composition of each objects. All the spectra are normalize at 0.55μm and are shifted by one unit for clarity. The spectra and models are 55565 (Doressoundiram *et al.* 2005a); 47171 (Dotto *et al.* 2003c); 38628 & 47932 (de Bergh *et al.* 2004); 90482 (de Bergh *et al.* 2005); 90377 (Barucci *et al.* 2005b) and 28978 (Boehnhardt *et al.* 2004).

2004), and (32532) 2001 Thereus (Barucci *et al.* 2002a) are modelled with geographical mixtures of tholins, ice tholin, amorphous carbon and water ice. The water ice bands in the spectrum of (28978) Ixion are somewhat uncertain. The spectrum of (38628) Huya (2000 EB_{173}) is modelled by a mixture of tholins, amorphous carbon, water ice, and jarosite (a hydrous iron sulfate) (de Bergh *et al.* 2004). The TNO spectra of 55565 2002 AW_{197} and those of the Centaurs 55576 2002 GB_{10} and 83982 2002 GO_9 are modelled by intimate mixtures of Triton tholins, amorphous carbon and contaminated water ices (intramixture). A high quality spectra has been obtained for the biggest objects, 90482 Orcus and 90377 Sedna. Orcus are modelled with geographical mixture of kerogen, amorphous carbon and water ice (Fornasier *et al.* 2004; de Bergh *et al.* 2005). Sedna, which is the most distant object has a surface composition completely different from the other TNOs with a total ice abundance >50% (Barucci *et al.* 2005b). Its composition resembles that of Triton, particularly in terms of presence of N_2 and CH_4. The presence of frozen nitrogen on Sedna implies that there is a thin atmosphere of nitrogen gas surrounding

https://doi.org/10.1017/S1743921305006733 Published online by Cambridge University Press

the approximately 200 years of its 10,500-years orbit when it is closest to the Sun. Jewitt & Luu (2004) observed recently Quaoar at Subaru telescope and detected the presence of crystalline water ice on its surface which could imply the existence of cryovolcanism.

A few objects such as 31824 (1999 UG_5), 19308 (1996 TO_{66}) and 32532 Thereus show surface variations (Merlin *et al.* 2005), but in some cases small spectral difference could be due to low quality data.

7. Conclusions

Even though more than 13 years have passed since the discovery of the first TNO, the knowledge of the TNOs' surface properties is still limited due to the faintness of these distant objects.

Surface color diversity is now confirmed by numerous surveys and the main results from statistical analysis are:

- Strong correlations between optical colors and orbital inclination and perihelion for Classical objects; these two correlations appear connected to each other and the color-perihelion correlation seems size dependent.
- Classical objects subdivide in two inclination groups (dynamically "hot" and "cold") at $i \sim 4.5°$; further studies are needed to clarify if the previous correlations are due to such subdivision.
- Plutinos possess an excess of small blue objects while Scattered Disk Objects a lack of red objects; no clear trends are detected among these dynamical groups.
- Centaurs separate in two visible color groups but there is no evidence of any clear trends with orbital parameters.
- Plutinos' and Centaurs' colors are statistically compatible with those of Scattered Disk Objects and Classical objects, though Scattered Disk Objects and Classical objects are not compatible.
- Colors of Short Period Comets and giant planets' irregular satellites are statistically compatible; irregular satellites are compatible with Scattered Disk Objects but such compatibility is not clear for Short Period Comets.
- Using robust multivariate statistical analysis, four taxonomic groups for TNOs and Centaurs has been obtained, namely: BB, BR, IR, and RR.

The wide diversity of color is confirmed by the different spectral behavior, even though only a few high-quality spectra exist. The spectra show:

- A large range of slope; some are featureless with almost constant gradients over the visible-NIR range, while some show absorption features of ices (most are H_2O);
- Three objects show features attributable to the presence of hydrous silicates, but this still needs to be confirmed;
- N_2 ice has been detected on the surface of the most distant object 90377 Sedna probably implying a thin atmosphere.

Radiative transfer models have been applied to the obtained spectral reflectance of TNOs and Centaurs, but each is subject to the limitations imposed by the quality of the astronomical spectra, the generally unknown albedo, and to the limited library of materials for which optical constants have been determined.

The models of red objects all use organic materials, such as tholins and kerogen, because common minerals (and ices) cannot provide a sufficiently red color.

H_2O ice is presumed to be the principal component of the bulk composition of outer Solar System objects, but it has been detected (generally with weak absorption) only on few objects. H_2O ice has to be present and could be hidden by low-albedo, opaque surface

https://doi.org/10.1017/S1743921305006733 Published online by Cambridge University Press

materials and for these reasons may appear only in few spectra. Additionally, various processes of space weathering (due to solar radiation, cosmic rays and interplanetary dust), can affect the uppermost surface layer and alter their surface chemistry.

The observed surface diversity can be due to different collisional evolutionary states and to different degrees of surface alteration due to space weathering. Collisions can rejuvenate the surface locally by excavating material from the subsurface.

New SPITZER observations will give an important contribution on the albedo knowledge and the NASA's New Horizons mission to the Kuiper Belt and Pluto-Charon, will offer the first close-up views of several solid bodies beyond Neptune.

Note added in proof: The discovery of three new objects – 2003 UB313, 2003EL61, and 2005 FY9 – have been announced at the epoch of ACM meeting. These are very big and 2003 UB313 seems even larger than Pluto. Observations from Gemini Observatory show that the near-infrared spectra of 2003 UB313 and 2005 FY9 are like that of Pluto dominated by the presence of frozen methane, while the spectrum of 2003 EL61 is dominated by crystalline water ice like Charon.

References

Barucci, M. A., Capria, M. T., Coradini, A., & Fulchignoni, M. 1987, Icarus, 72, 304

Barucci, M. A., Romon, J., Doressoundiram, A., & Tholen, D. J. 2000, Astron. J., 120, 496

Barucci, M. A., Fulchignoni, M., Doressoundiram, A., & Birlan, M. 2001, Astron. Astrophys., 471, 1150

Barucci, M. A., Boehnhardt, H., Dotto, E., *et al.* 2002a, Astron. Astrophys., 392, 335

Barucci, M. A., Cruikshank, D. P., Mottola, S., & Lazzarin, M. 2002b, Asteroids III, ed. W. F., Bottke, A., Cellino, P., Paolicchi, & R. P., Binzel, 273

Barucci, M., Doressoundiram, A., & Cruikshank, D. 2004, in Comets II, ed. M. Festou, H. Keller, & H. Weaver, 647

Barucci, M., Belskaya, I., Fulchignoni, M., & Birlan, M. 2005a, Astron. J., 130, 1291

Barucci, M., Cruikshank, D., Dotto, E., *et al.* 2005b, Astron. Astrophys., 439, L1

Bauer, J. M., Meech, K. J., Fernández, Y. R., Farnham, T. L., & Roush, T. L. 2002, Publ. Astron. Soc. Pac., 114, 1309

Bauer, J. M., Fernández, Y. R., & Meech, K. J. 2003, Publ. Astron. Soc. Pac., 115, 981

Belskaya, I. N., Barucci, A. M., & Shkuratov, Y. G. 2003, Earth Moon and Planets, 92, 201

Bernstein, G. M., Trilling, D. E., Allen, R. L., *et al.* 2004, Astron. J., 128, 1364

Boehnhardt, H., Tozzi, G. P., Birkle, K., *et al.* 2001, Astron. Astrophys., 378, 653

Boehnhardt, H., Bagnulo, S., Muinonen, K., *et al.* 2004, Astron. Astrophys., 415, L21

Brown, R. H., Cruikshank, D. P., Pendleton, Y. J., & Veeder, G. J. 1997, Science, 276, 937

Brown, M. E. 2001, Astrophys. J., 121, 2804

Brown, M. & Trujillo, C. 2004, Astrophys. J., 127, 2413

Cooper, J. F., Christian, E. R., Richardson, J. D., & Wang, C. 2003, Earth Moon and Planets, 92, 261

Cruikshank, D. P., Roush, T. L., Bartholomew, M. J., *et al.* 1998, Icarus, 135, 389

de Bergh, C., Boehnhardt, H., Barucci, M. A., *et al.* 2004, Astron. Astrophys., 416, 791

de Bergh, C., Delsanti, A., Tozzi, G., *et al.* 2005, Astron. Astrophys., 437, 1115

Delsanti, A., Hainaut, O., Jourdeuil, E., *et al.* 2004, Astron. Astrophys., 417, 1145

Doressoundiram, A., Barucci, M., Romon, J., & Veillet, C. 2001, Icarus, 154, 277

Doressoundiram, A., Peixinho, N., de Bergh, C., *et al.* 2002, Astron. J., 124, 2279

Doressoundiram, A., Tozzi, G. P., Barucci, M. A., *et al.* 2003, Astrophys. J., 125, 2721

Doressoundiram, A., Barucci, M. A., Tozzi, G. P., *et al.* 2005a, Planet. Space Sci. (in press)

Doressoundiram, A., Peixinho, N., Doucet, C., *et al.* 2005b, Icarus, 174, 90

Dotto, E., Barucci, M. A., Boehnhardt, H., *et al.* 2003a, Icarus, 162, 408

Dotto, E., Barucci, M. A., Boehnhardt, H., *et al.* 2003b, Icarus, 162, 408

Dotto, E., Barucci, M. A., Leyrat, C., *et al.* 2003c, Icarus, 164, 122
Fornasier, S., Doressoundiram, A., Tozzi, G. P., *et al.* 2004, Astron. Astrophys., 421, 353
Fulchignoni, M., Birlan, M., & Antonietta Barucci, M. 2000, Icarus, 146, 204
Gomes, R. S. 2003, Icarus, 161, 404
Grundy, W. M., Noll, K. S., & Stephens, D. C. 2005, Icarus, 176, 184
Hainaut, O. R. & Delsanti, A. C. 2002, Astron. Astrophys., 389, 641
Hartigan, J. A. & Hartigan, P. M. 1985, Ann. Stat., 13, 70
Horner, J., Evans, N. W., & Bailey, M. E. 2004, Mon. Not. R. Astron. Soc., 354, 798
Howell, S. B. 1989, Publ. Astron. Soc. Pac., 101, 616
Jewitt, D. & Luu, J. 1993, Nature, 362, 730
Jewitt, D. C. & Luu, J. X. 2001, Astron. J., 122, 2099
Jewitt, D. 2002, Astron. J., 123, 1039
Jewitt, D. C. & Luu, J. 2004, Nature, 432, 731
Lacerda, P. & Luu, J. 2005, Astrophys. J. (submitted)
Lamy, P., Toth, I., Fernández, Y., & Weaver, H. 2005, in Comets II, ed. M. Festou, H. Keller, & H. Weaver, 223
Lazzarin, M., Barucci, M. A., Boehnhardt, H., *et al.* 2003, Astrophys. J., 125, 1554
Levison, H. F. & Duncan, M. J. 1997, Icarus, 127, 13
Levison, H. F. & Stern, S. A. 2001, Astrophys. J., 121, 1730
Luu, J. & Jewitt, D. 1996a, Astron. J., 112, 2310
Luu, J. & Jewitt, D. C. 1996b, Astron. J., 111, 499
McBride, N., Green, S. F., Hainaut, O., & Delahodde, C. 1999, in Asteroids, Comets, and Meteors 1999 Abstracts Volume
Merlin, F., Barucci, M., Dotto, E., de Bergh, C., & Lo Curto, G. 2005, Astron. Astrophys. (in press)
Morbidelli, A., Brown, M. E., & Levison, H. F. 2003, Earth Moon and Planets, 92, 1
Moroz, L. V., Baratta, G., Distefano, E., *et al.* 2003, Earth Moon and Planets, 92, 279
Mueller, B. E. A., Hergenrother, C. W., Samarasinha, N. H., Campins, H., & McCarthy, D. W. 2004, Icarus, 171, 506
Peixinho, N., Doressoundiram, A., Delsanti, A., *et al.* 2003, Astron. Astrophys., 410, L29
Peixinho, N., Boehnhardt, H., Belskaya, I., *et al.* 2004, Icarus, 170, 153
Peixinho, N. 2005, PhD Thesis, University of Lisbon
Romon-Martin, J., Barucci, M. A., de Bergh, C., *et al.* 2002, Icarus, 160, 59
Romon-Martin, J., Delahodde, C., Barucci, M. A., de Bergh, C., & Peixinho, N. 2003, Astron. Astrophys., 400, 369
Russell, H. N. 1916, Astrophys. J., 43, 173
Sheppard, S. S. & Jewitt, D. C. 2002, Astrophys. J., 124, 1757
Stetson, P. B. 1990, Publ. Astron. Soc. Pac., 102, 932
Strazzula, G., Cooper, J., Christian, E., & Johnson, R. E. 2003, Comptes Rendus de l'Académie des Sciences, Tome 4, Fascicule 7, 791
Tegler, S. C. & Romanishin, W. 1998, Nature, 392, 49
Tegler, S. & Romanishin, W. 2000, Nature, 407, 979
Tegler, S. & Romanishin, W. 2003, Icarus, 161, 181
Tegler, S. C., Romanishin, W., & Consolmagno, S. J. 2003, Astrophys. J., Lett., 599, L49
Thébault, P. & Doressoundiram, A. 2003, Icarus, 162, 27
Tholen, D. 1984, PhD thesis, University of Arizona, Tucson
Tholen, D. J. & Barucci, M. A. 1989, in Asteroids II, 298–315
Trujillo, C. A. & Brown, M. E. 2002, Astrophys. J., Lett., 566, L125
Trujillo, C. A. & Brown, M. E. 2003, Earth Moon and Planets, 92, 99
Vilas, F. & Gaffey, M. J. 1989, Science, 246, 790
Yu, Q. & Tremaine, S. 1999, Astrophys. J., 118, 1873